ISSN : 0974 - 7486 Volume 9 Issue 3

Trade Science Inc.

Materials Science

An Indian Journal

Full Paper

MSAIJ, 9(3), 2013 [107-112]

Mechanical and electrochemical properties of a cast carbon steel. Part 1: Behaviour in compression and hardness

Elodie Conrath[1], Patrice Berthod[2]

[1]Faculty of Sciences and Technologies, B.P. 70239, 54506 Vandoeuvre-lès-Nancy, (FRANCE)

[2]Institut Jean Lamour (UMR CNRS 7198), department CP2S

University of Lorraine, B.P. 70239, 54506 Vandoeuvre-lès-Nancy, (FRANCE)

E-mail: patrice.berthod@univ-lorraine.fr

ABSTRACT

In some cases carbon steels can be shaped by plastic deformation with as result a heterogeneous repartition of hardening effects and different surface corrosion behaviours, the two depending on the local deformation mode as well as on the local deformation rate. To complete previous works concerning other compositions of steel and other modes of plastic deformation, a ferrito-pearlitic steel was here elaborated by foundry and shaped as a cylinder by using a special foundry technique, then cut into samples to which different rates of plastic deformation were applied by compression. A not-deformed cylindrical sample and the other cylindrical samples having been subjected to compression were cut in order to generate two types of samples, metallographic samples for microstructure examination + Vickers indentation and electrodes for a later corrosion study, characterized by two main orientations with respect to the deformation direction. In this first part only the microstructures and hardness levels are of interest. It is found that hardness increases more or less by comparison to the not-deformed state, this depending on the considered orientation. The comparison with previous works shows that this increase depends on the chemical composition of the steel, on the deformation rate and on the orientation, but also that the order between the two orientations depends on the steel type and on the deformation mode.

KEYWORDS

Carbon steel;
Compression behaviour;
Plastic deformation;
Deformed microstructure;
Hardness.

INTRODUCTION

The forming of metallic alloys by plastic deformation at low temperature or at higher temperature modifies significantly their microstructures[1]. These microstructural consequences of hardening can be easily revealed during metallographic observations: initial equiaxed structure converted in a new one displaying special orientations, phases obviously deformed, grain elongation ... Many works have since long time demonstrated that it generally results some modifications of properties for the concerned alloys, in the mechanical field[2,3] as well as for other properties very different such as some magnetic ones[4]. Concerning the mechanical properties some changes may be found for tensile, compression or shear strength or hardness, for

instance, as this occurs for not-alloyed or highly alloyed steels, copper alloys, aluminium alloys ... after cold- or hot-rolling[5], extrusion[6], plastic torsion deformation[7]. These properties may have lost their initial isotropic character (if any), as consequences of the orientated nature of these deformations.

In this work, a carbon steel was especially elaborated by casting following a special method which allows obtaining cylindrical ingots with a solidification progress characterized by a revolution symmetry. Different levels of deformation were reproduce by compression along the ingot axis for studying the corrosion behaviour of the compressed samples. In this first part of the work the mechanical behaviour in compression of the steel is studied, while the corrosion results will be presented in a second part.

EXPERIMENTAL

Elaboration of the alloys

The carbon steel was obtained by casting with a cylindrical shape for the ingot (diameter: 10mm, length: about four centimetres) by using the same method as in a recent study[8]. Small parts of pure iron and of carbon (total mass: about 50g) were melted together in a CELES high frequency induction Furnace until a molten ball (in levitation due to the electromagnetic field) was obtained. A silica tube with an internal diameter of 10mm was then introduced in the levitating liquid to aspire with a vacuum pump the greatest part of the later one in the tube where it is solidified with a solidification progress from the internal cylindrical wall of the silica tube towards the tube axis. This cylindric ingot was then cut by using a precision cutter Isomet 5000 (Buelher), to obtain several cylindrical samples of about one centimetre long. A first one was kept and was not subjected to mechanical deformation while the others were thereafter tested in compression by targeting different rates.

Compression runs

The compression tests were run by subjecting the concerned samples to an increasing force applied by a MTS RF/150 machine equipped with two compression platens and a force cell of capacity equal to 150kN (Figure 1). The compressive deformation was applied

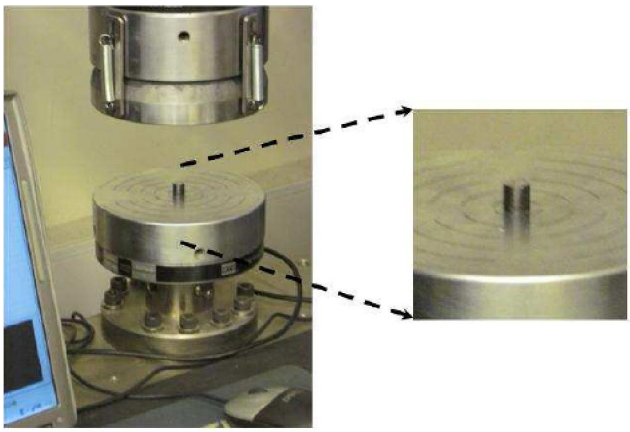

Figure 1 : The compression platens and the cylindrical sample which will be compressed

in the direction of the ingot axis, with a speed of 0.25 mm/min. It was manually stopped when the desired deformation rates were obtained. The new heights of the deformed samples were, as for the initial heights, measured with a high precision numerical calliper, and the corresponding relative plastic deformations were then calculated.

Metallographic samples preparation and hardness measurements

Parts cut in the not-deformed samples and in the compressed samples were destined to prepare metallographic samples. After having been embedded in a cold resin mixture (ESCIL: Araldite CY230 and hardener HY 956), they were polished with SiC papers up to 1200 grit, then ultrasonically cleaned. A final polishing, achieved with textile support enriched in 1µm-alumina particles, led to a mirror-like state.

The polished samples were first subjected to X-ray diffraction (XRD) performed with a Philips X'Pert Pro diffractometer. An etching by immersion during about ten seconds in a "Nital4" solution (ethylic alcohol with 4% of pure nitric acid) at room temperature allowed examining the as-cast and deformed microstructures. At least three indentations were achieved on the metallic surfaces of the {embedded + polished} samples, with a Testwell Wolpert machine. The average value and the standard deviation were then calculated, for all the deformed states and for the two orientations with respect to the sample (or compression) axis.

RESULTS AND DISCUSSION

Compression tests

Three samples were compressed. With the first one a deformation of -9.19% was obtained (maximal stress applied: 607 MPa) while, with the second one, a deformation of 7.15% (maximal stress: 620 MPa) was obtained in a first time but this second sample was thereafter compressed again to obtain a final deformation of -20.25% (maximal stress: 859 MPa). The initial and final dimensions of the compressed samples are given in TABLE 1.

TABLE 1 : Dimensional evolution of the samples during the one step first compression and the two-steps second compression

Relative height deformation	Initial dimensions (mm)		Final dimensions (mm)	
	height	diameter	height	diameter
-9.19%	8.19+/- 0.05	10.87 +/- 0.03	7.44 +/- 0.00	11.28 +/- 0.01
-7.13% (1st run)	6.88 +/- 0.02	10.88 +/- 0.03	6.39 +/- 0.01	11.30 +/- 0.06
-20.25% (2nd run)			5.48	12.32

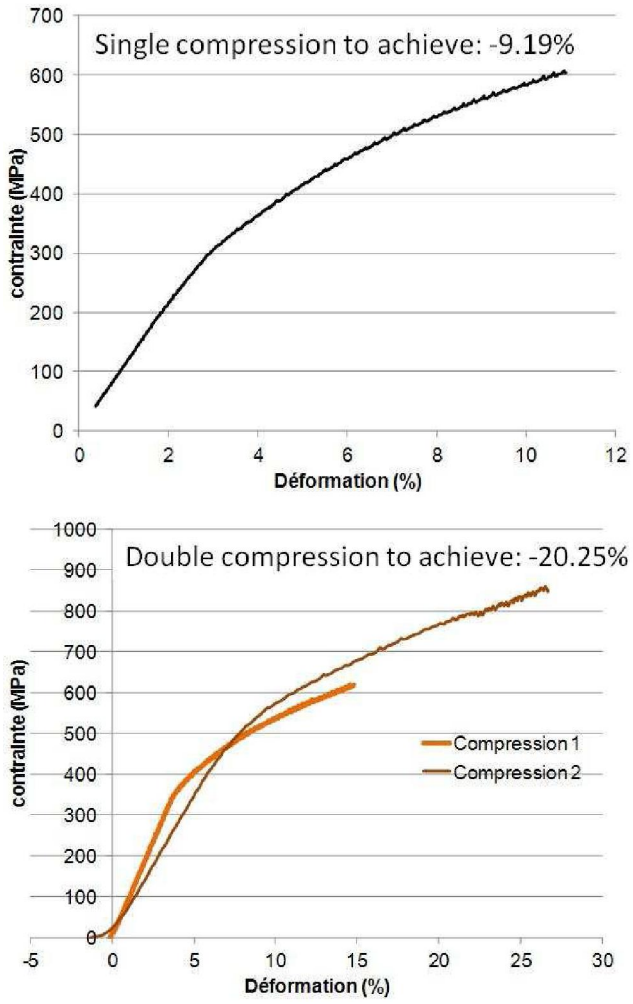

Figure 2 : The stress curve recorded during the first compression test leading to a permanent deformation of -9.19% and the two successive curves of the compression test leading to -20.25%

The corresponding stress versus deformation (not real deformation but deformation calculated with the traverse movement) curves are shown in Figure 2.

On these curves the Young's modulus cannot be assessed since no extensometer was used. In contrast it is possible to extract the maximal elastic tensile stress (at which the linear Hooke's law begins to be lost): this one was 231MPa for the first curve (which led to -9.19% of final relative deformation), and 334 MPa and 344 MPa for, respectively, the first part and the second part of the second compression test (the total leading to -20.25% of final relative deformation). The obtained samples were photographed in Figure 3 (-9.19%) and in Figure 4 (-20.25%), illustration allowing to see the decrease in height and the lateral enlargement in average diameter, by compression.

The not compressed sample and the two deformed samples were cut following a procedure which allows

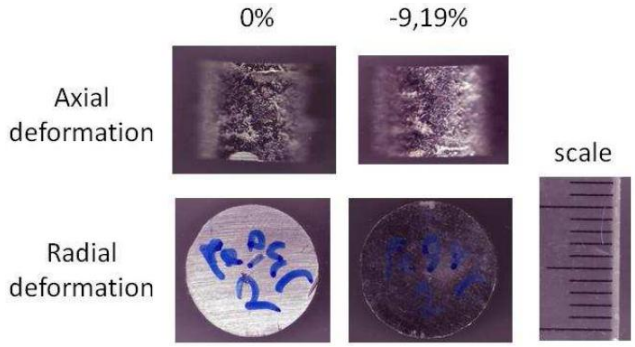

Figure 3 : Photographs of the first sample before and after deformation

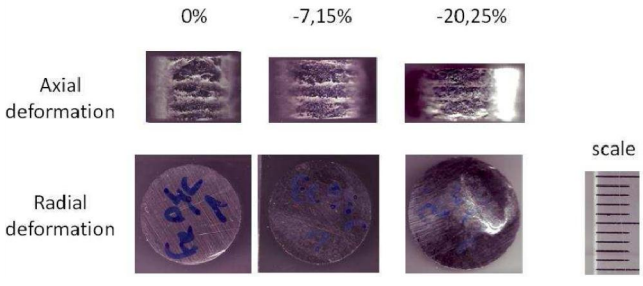

Figure 4 : Photographs of the second sample before deformation, after the first compression and after the second compression

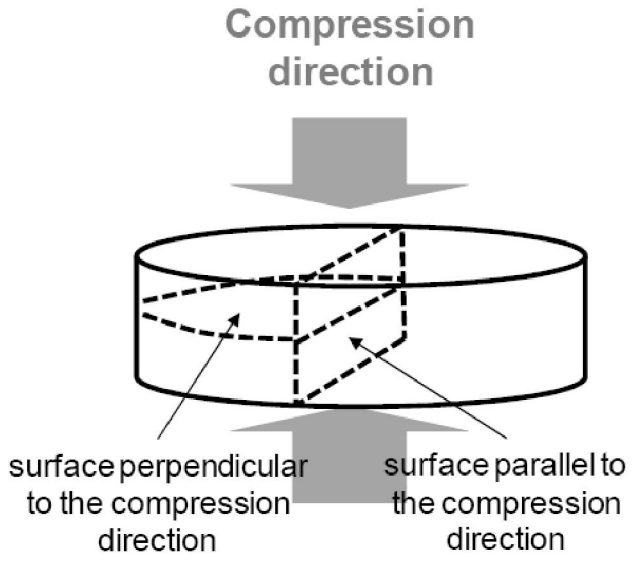

Figure 5 : Cutting method to obtain samples for XRD runs and metallographic samples for the observation of their microstructures (not-deformed steel and compressed steels)

obtaining samples for embedding and polishing, then for X-ray diffraction characterization and microstructure examinations (Figure 5).

The X-Ray diffraction runs led to spectra which do not reveal any modification for the diffraction peaks (Figure 6 for the parallel orientation and Figure 7 for the perpendicular one). It appears that there are no modifications between the not-deformed state and the two deformed ones, neither for the parallel orientation, nor for the perpendicular one, and no difference too between the two orientations for a given deformed state. The peaks correspond to the crystalline lattice of BCC

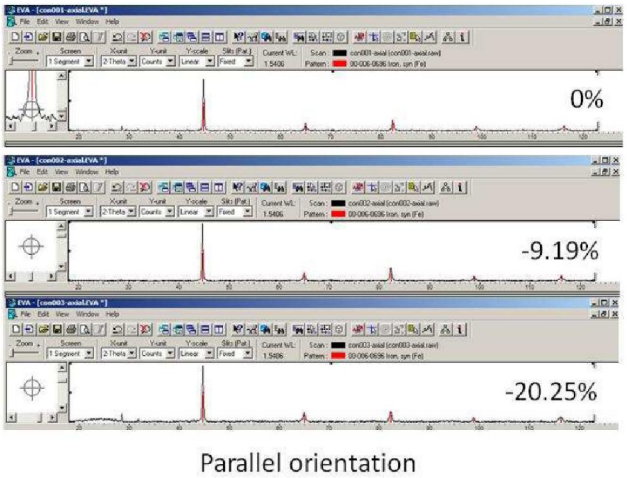

Figure 6 : XRD patterns for the parallel orientation (for the not-compressed sample (top) and for the two deformed samples)

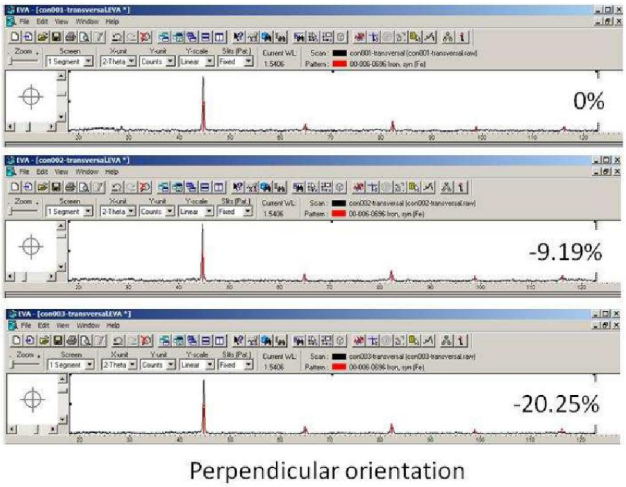

Figure 7 : XRD patterns for the perpendicular orientation (for the not-compressed sample (top) and for the two deformed samples)

ferrite which is the main phase present in volume fraction in this ferrito-pearlitic steel.

The microstructures of the three samples for the two orientations are displayed in Figure 8. The ferrito-pearlitic microstructures (of a particular type resulting of the special conditions of solidification and post-solidification cooling (solid state transformations) due to the aspiration in silica tube before solidification, illustrate – especially for the most deformed state and the parallel orientation – the effect of compression at the microscopic scale.

Vickers indentations were performed on all the six metallographic samples, leading to the results graphically presented in Figure 9. One can see that the hardness logically increases with the plastic deformed rate of the sample, but only for the perpendicular orientation. Indeed the hardness remains almost constant for the other orientation although it seems having a slight tendency to increase too.

General commentaries

The elaboration method allowed thus obtaining a cylindrical ingot, fortunately free of axial shrinkage defects, long enough to permit cutting easily several cylindrical ingots of the same chemical composition. The compression tests allowed specifying the maximal stress at which the purely elastic deformation begins to become plastic. The values obtained are rather close another and typical of the values range usually encountered for Re for such ferrito-pearlitic carbon steels.

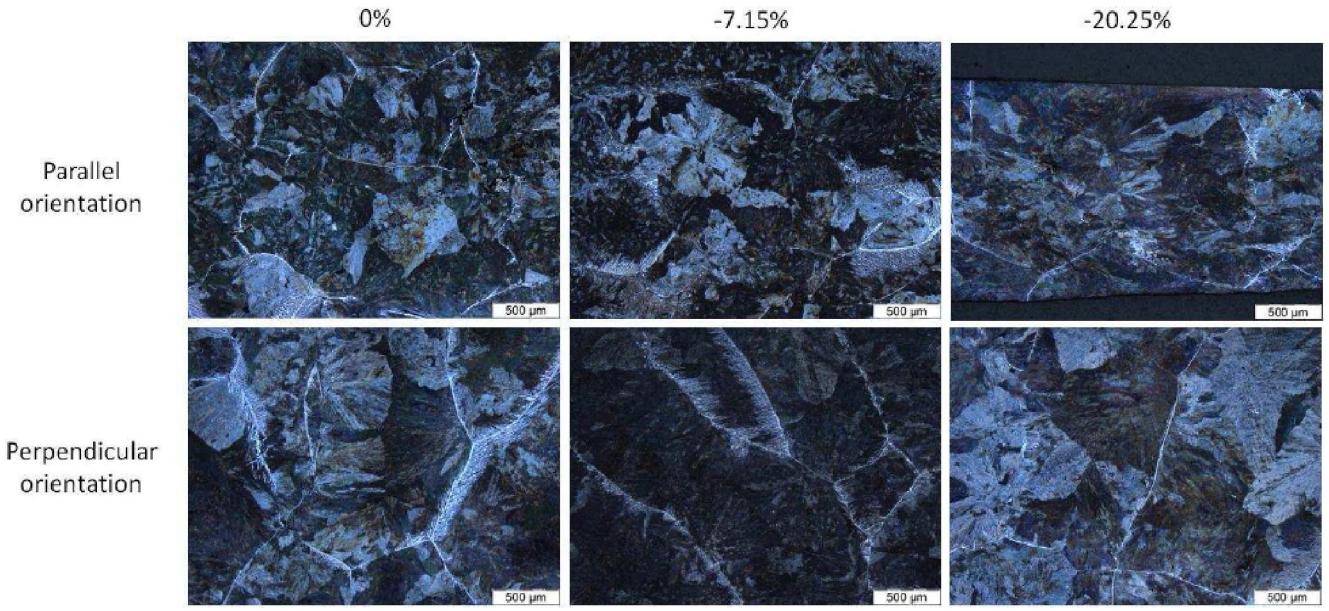

Figure 8 : Visualization of the deformation at the microstructure scale (after Nital4 etching); this is particularly evidenced for the {parallel orientation – highest rate} in the {top-right} micrograph

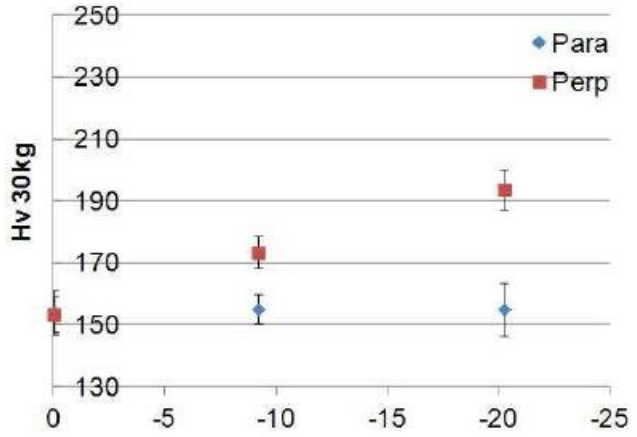

Figure 9 : Hardness evolution with the deformation rate and for the two orientations with respect to the deformation axis

However there is a noticeable difference of the Re value obtained for the first sample and the two ones obtained for the second sample (which are higher than the previous one). It is possible that the determination of the loss of linearity was more difficult to do since no compression-devoted extensometer was available for obtaining much more accurate (notably not so important) values for the deformation of the samples only. The Vickers-indentation values clearly showed an increase of hardness for the plastically deformed (thus hardened) alloy, but much more for the perpendicular orientation than for the parallel one which seems to be much less dependent on the plastic deformation rate (maybe a very low increase with the deformation rate). Since the values for the two orientations were quite similar, the hardness for the perpendicular orientation became, when the deformation rate increased, more and more superior to for the parallel orientation. This merits to be compared to previous results as the orientation-dependence of hardness for a ferritic steel deformed in traction[12] and for a ferrito-pearlitic steel deformed in traction too[13]. In the first case one can remind that the hardness (Vickers too) increased, from about 100Hv (for the two orientations, typical of ferrite) faster for the parallel orientation than for the perpendicular one. In the second case hardness increased, from about 185Hv with the deformation rate for both orientations, a little faster for the perpendicular orientation than for the other one. In the present case, the elaboration of the steel is different and the hardening achieved by compression instead by traction. In all the three cases the hardness globally increases but the hierarchy between the two orientation obviously depends on the carbon content (microstructure rating between ferrite and pearlite) and on the type of uniaxial deformation.

CONCLUSIONS

The deformation in compression of the studied carbon steel allowed obtaining samples which were here characterized in term of hardness, results coming completing a set of previous data concerning also carbon

steels but with other carbon contents and also concerning the opposite type of deformation: tensile strain. The other parts of the same ingots, a one parallel to deformation and a one perpendicular, for each state of deformation are reserved to electrochemical tests for evaluating the corrosion behaviour[14], to here complete recent data in this field concerning a ferritic steel and a stainless austenitic one[15].

REFERENCES

[1] J.M.Dorlot, J.P.Baïlon, J.Masounave; Des Matériaux, Editions de l'ecole polytechnique de montréal, Montréal, **(1986)**.

[2] Y.D.Koryagin, N.T.Kareva, M.A.Smirnov; Physics of Metals and Metallography, **55**, 187 **(1983)**.

[3] V.G.Serebryakpv, E.I.Ehstrin; Fizika Metallov I Metallovedenie, **2**, 130 **(1992)**.

[4] A.H.Qureshi, L.N.Chaudhary; Journal of Applied Physics, **41**, 1042 **(1970)**.

[5] E.L.Svistunova, A.A.Gulyaev, A.B.Oralbaev; Fizika Metallov I Metallovedenie, **78**, 108 **(1994)**.

[6] J.Zdunek, P.Widlicki, H.Garbacz, J.Mizera, K.J.Kurzydlowski; Diffusion and defect data Pt.B: Solid State Phenomena, **114**, 171 **(2006)**.

[7] A.V.Korzinkov, Y.V.Ivanisenko, D.V.Laptionok, I.M.Safarov, V.P.Pilyugin, R.Z.Valiev; Nanostructured Materials, **4**, 159 **(1994)**.

[8] P.Y.Girardin, A.Frigerio, P.Berthod; Materials Science: An Indian Journal, submitted.

[9] M.Durand-Charre; Microstructure of steels and cast irons, Springer Verlag, Berlin, **(2004)**.

[10] L.E.Samuels, T.O.Mulhearn; Journal of The Mechanics and Physics of Solids, **5(2)**, 125 **(1957)**.

[11] B.Karlsson, G.Linden; Materials Science and Engineering, **17(2)**, 209 **(1975)**.

[12] S.De Sousa, P.Berthod, J.P.Philippe; Materials Science: An Indian Journal, **6(3)**, 170 **(2010)**.

[13] P.Berthod, S.De Sousa, J.P.Philippe; UPB Scientific Bulletin Series B, **73(1)**, 173 **(2011)**.

[14] P.Berthod, E.Conrath; Materials Science: An Indian Journal, to be submitted.

[15] P.Y.Girardin, A.Frigerio, P.Berthod; Materials Science: An Indian Journal, submitted.